INSTITUTE OF PHYSICS PUBLISHING PHYSICS IN MEDICINE AND BIOLOGY

Phys. Med. Biol. **49** (2004) 1915–1932 PII: S0031-9155(04)65223-7

Automatic beam angle selection in IMRT planning using genetic algorithm

Yongjie Li[1,2], Jonathan Yao[2] and Dezhong Yao[1]

[1] School of Life Science and Technology, University of Electronic Science and Technology of China, Chengdu 610054, People's Republic of China
[2] Topslane Inc., Pleasant Hill, CA 94523, USA

E-mail: dyao@uestc.edu.cn

Received 25 June 2003
Published 29 April 2004
Online at stacks.iop.org/PMB/49/1915
DOI: 10.1088/0031-9155/49/10/007

Abstract

The selection of suitable beam angles in external beam radiotherapy is at present generally based upon the experience of the human planner. The requirement to automatically select beam angles is particularly highlighted in intensity-modulated radiation therapy (IMRT), in which a smaller number of modulated beams is hoped to be used, in comparison with conformal radiotherapy. It has been proved by many researchers that the selection of suitable beam angles is most valuable for a plan with a small number of beams ($\leqslant 5$). In this paper an efficient method is presented to investigate how to improve the dose distributions by selecting suitable coplanar beam angles. In our automatic beam angle selection (ABAS) algorithm, the optimal coplanar beam angles correspond to the lowest objective function value of the dose distributions calculated using the intensity-modulated maps of this group of candidate beams. Due to the complexity of the problem and the large search space involved, the selection of beam angles and the optimization of intensity maps are treated as two separate processes and implemented iteratively. A genetic algorithm (GA) incorporated with an immunity operation is used to select suitable beam angles, and a conjugate gradient (CG) method is used to quickly optimize intensity maps for each selected beam combination based on a dose-based objective function. A pencil-beam-based three-dimensional (3D) full scatter convolution (FSC) algorithm is employed for the dose calculation. Two simulated cases with obvious optimal beam angles are used to verify the validity of the presented technique, and a more complicated case simulating a prostate tumour and two clinical cases are employed to test the efficiency of ABAS. The results show that ABAS is valid and efficient and can improve the dose distributions within a clinically acceptable computation time.

1. Introduction

Intensity-modulated radiation therapy (IMRT) has gained more and more attention because of its advantage of producing a highly three dimensional conformal dose distribution to the target, while sparing organs at risk (OARs) and normal tissues. Compared with traditional three-dimensional conformal radiation therapy (3D-CRT) that conforms only two dimensionally to the target projection in the plane perpendicular to the beam orientation, IMRT can significantly improve the outcome of radiation therapy. Many efforts have been made to make IMRT an easy implementation through increasing the automatization of beam set-up, shortening the optimization time of inverse planning, enhancing the ability of dose verification, and so on (Webb 2000).

The selection of suitable beam angles in external beam radiotherapy is at present generally based upon the experience of the human planner. Normally several trial-and-error attempts are needed in order to find a group of adequate beam angles. Although this leads to good treatment plans, they are not necessarily optimal (Rowbottom *et al* 1998a). Computer optimization of the beam directions has the potential to achieve optimal plans that are customized for each individual patient. The requirement to automatically select beam angles is particularly highlighted in IMRT, in which a smaller number of modulated beams is hoped to be used, in comparison with conformal radiotherapy, in order to shorten the treatment time. It has been proved by many researchers that the selection of suitable beam angles is most valuable for a plan with a small number of beams ($\leqslant 5$) (Bortfeld and Schlegel 1993, Soderstrom and Brahme 1995, Stein *et al* 1997, Rowbottom *et al* 1998a, 1998b, 2001, Pugachev *et al* 2000). The ultimate goal of the beam angle optimization is to achieve the best possible dose distribution by using the minimum number of beams (Pugachev *et al* 2000).

The problem of selection of suitable beam directions in external beam radiation therapy was studied as early as 1992 by Soderstrom and Brahme. They proposed entropy and Fourier transform measures for the selection of suitable beam orientations. Bortfeld and Schlegel (1993) used simulated annealing to optimize the beam directions in the frequency domain. Their general conclusion is that the optimal beam configuration for multiple-beam irradiations (with more than three beams) tends to be an even distribution over an angular range of 0 to 2π, whereas it is very important to optimize the beam directions when the number of beams is only two or three. They also concluded that it is not in general useful to avoid beam orientations through organs at risk for modulated beams. Similar conclusions have also been made by Soderstrom and Brahme (1995), Stein *et al* (1997), Rowbottom *et al* (1998a, 1998b, 2001) and Pugachev *et al* (2000).

The genetic algorithm (GA), as a powerful global optimization approach, has been introduced by many researchers to solve radiation optimization problems. Ezzell (1996) used GA to find an optimal combination of external beams. Langer *et al* (1996) used GA to optimize the beam weights for treatment of abdominal tumours. Yu and Schell (1996) chose GA for the optimization of prostate implants. Wu and Zhu (2000) proposed a technique to optimize the beam directions and weights using a mixed-encoding GA. Zhang *et al* (2001) used a hybrid algorithm called guided evolutionary simulated annealing (GESA), which combined the GA and SA together, to optimize the gamma knife treatment planning. Despite the drawback of extensive computation, similar to simulated annealing, the potential of GA is very attractive.

In this paper, a new efficient technique is developed to implement automatic beam angle selection (ABAS). In ABAS a specified number of angle candidates are selected from a discrete angle candidates pool using a GA, and then the intensity maps of these angles are optimized using a conjugate gradient (CG) method under the guidance of a dose-based objective function.

After a great number of iterations (generations), the angle combination with the highest fitness value is regarded as giving the optimal beam angles for the case. A final refined beam intensity map optimization is performed using these optimal beam angles, under the guidance of a more complicated dose–volume-based objective function. In section 3 two simulated test cases with obvious optimal beam angles are used to verify the validity of the presented technique, and a more complicated case simulating a prostate tumour and two clinical cases are employed to test the efficiency of ABAS. The results show that ABAS is valid and efficient and can improve the dose distributions within a clinically acceptable computation time.

2. Materials and methods

2.1. Objective function

A whole form of the objective function used in this paper can be written as

$$F_{\text{obj}}(\vec{x}^{(k)}) = \alpha \cdot F_{\text{OAR}}(\vec{x}^{(k)}) + \beta \cdot F_{\text{PTV}}(\vec{x}^{(k)}) \tag{1}$$

$$F_{\text{OAR}}(\vec{x}^{(k)}) = \sum_{i=1}^{N_{\text{OAR}}} \sum_{j=1}^{NT_i} \delta \cdot w_j \cdot (d_j(\vec{x}^{(k)}) - p_j)^2 \tag{2}$$

$$\begin{aligned} F_{\text{PTV}}(\vec{x}^{(k)}) = {} & \gamma \cdot \sum_{j=1}^{NT_{\text{PTV}}} \delta \cdot w_j \cdot \left(d_j(\vec{x}^{(k)}) - p_j\right)^2 \\ & - \eta \cdot \sum_{j=1}^{NT_{\text{PTV}}} \delta \cdot w_j \cdot \left(d_j(\vec{x}^{(k)}) - p_j - d_j(\vec{x}^{(k)}) \cdot \log\left(\frac{d_j(\vec{x}^{(k)})}{p_j}\right)\right) \end{aligned} \tag{3}$$

$$d_j(\vec{x}^{(k)}) = \sum_{m=1}^{N_{\text{ray}}} a_{jm} \cdot \vec{x}_m^{(k)}. \tag{4}$$

Here $F_{\text{OAR}}(\vec{x}^{(k)})$ is the part associated with all the OARs, $F_{\text{PTV}}(\vec{x}^{(k)})$ is the part associated with the target, N_{OAR} is the total number of OARs, NT_i is the point number in the ith OAR, NT_{PTV} is the point number in the target, $\delta = 1$ when the point dose in the volume breaks the constraints, else $\delta = 0$, w_j is the weight of the jth point, d_j is the calculated dose of the jth point in the volume, p_j is the prescribed dose of the jth point in the volume, a, β are the regularizing factors that control the importance between target and OARs, γ, η are the importance factors of the first and second parts in equation (1), N_{ray} is the total ray (also called pencil beam) number, a_{jm} is the dose deposited at the jth point from a unit weight of the mth ray, $\vec{x}_m^{(k)}$ is the intensity of the mth ray.

The second part in equation (3) is used to measure the homogeneity of dose distribution in the target through the entropy information (Wu and Zhu 2002). According to the information theory, maximum entropy is equivalent to minimizing information in the system, i.e. to maximize the homogeneity of dose distribution.

In our objective function both dose and dose–volume constraints are embedded. A dose constraint for the target is expressed as 'all doses should be higher than $D_{D\max}$ and lower than $D_{D\min}$', and a dose–volume constraint for the target is expressed as 'no more than $V_{\min}\%$ of the target volume can absorb doses lower than $D_{DV\min}$'. For the OARs, a dose constraint is denoted as 'all doses should be lower than $D_{D\max}$', and a dose–volume constraint is denoted as 'no more than $V_{\max}\%$ of the volume can absorb doses higher than $D_{DV\max}$'. The dose–volume

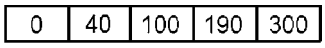

Figure 1. A chromosome with five genes (i.e. five beam angles): 0°, 40°, 100°, 190° and 300°.

constraints are realized through the penalty of those points breaking $V_{\max}\%$ or $V_{\min}\%$ after sorting the doses in ascending or descending order.

During the optimization of beam angles, the part associated with entropy measurement in the objective function is not involved, and also those dose–volume constraints are skipped in order to simplify the calculation. This is just a simple but popularly used dose-based quadratic objective function. Whereas the whole form of the objective function is employed to optimize the final intensity maps at those optimal angles using CG method.

2.2. Beam angle selection using the genetic algorithm

2.2.1. The genetic algorithm. The genetic algorithm (GA) is a global optimization technique that simulates the natural process of evolution in which the fittest solutions survive after numerous generations of natural selection and genetics (Goldberg 1989). Usually, an unknown variable in a solution is represented as a gene in a chromosome, and a solution with many variables is represented as a chromosome (also named *individual*). This process is called coding. Fitness is defined for each individual to evaluate its goodness. During the optimization process, GA keeps a group of candidate individuals (solutions) in each generation. Through genetic operations, such as selection, crossover and mutation, those individuals with better fitness will be propagated to the next generation with higher probability. After numerous generations of genetics, the individual with the best fitness among the last population is regarded as the optimal solution.

2.2.2. Coding scheme of GA. In this study a one-dimensional integer-coding scheme is adopted, in which the combination of beam angles is represented by a chromosome (an individual) with a length of user-specified beam number for the plan, and each gene in the chromosome represents a trial beam angle. Figure 1 shows a chromosome with five genes (i.e. five beam angles): 0°, 40°, 100°, 190° and 300°. The genes in one chromosome are different from each other, which means that there should be no two beams with the same angles in one plan.

2.2.3. Determination of the angle search space. The beams in this study are restricted to coplanar ones. To reduce the search space covering the total 2π gantry rotational angle, some beam angles that cannot be used because of the physical limitation or potential danger for treatment are specified by planners or by a knowledge-based database. Then the angle space excluding the discarded ranges is divided into equally spaced directions with a given angle step, such as 5° or 10°. There are three main situations for beam angle restriction: (1) beam orientations that would result in a collision between the treatment gantry and the patient couch; (2) beam orientations passing through the OARs that have a extra low radiation tolerance, e.g. the lens of the eye (Rowbottom *et al* 2001); and (3) beam orientations directly passing the metal frames of the patient couch or immobilizing couch that can heavily attenuate radiation.

Figure 2 shows an interactive tool for defining angle constraints in order to reduce the search space of beam angle optimization. There are two orientation constraints defined so that

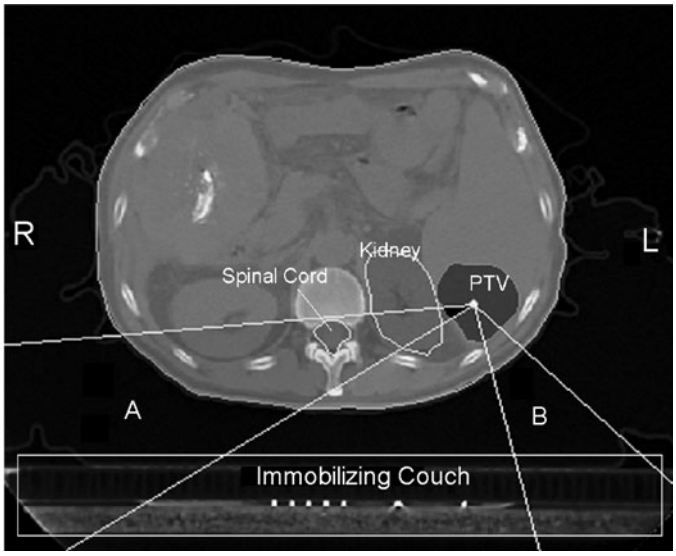

Figure 2. An interactive tool for defining angle constraints.

no beam is allowed to pass through. Constraint *A* is defined to protect the spinal cord and to avoid the right-hand side of the metal frame of the immobilizing couch, and constraint *B* is defined to avoid the left-hand side of the metal frame of the immobilizing couch.

2.2.4. Initialization of the first generation. The population size (i.e. the individual number in one generation), NP_{size}, is empirically set to double the total number of angle candidates (Wu and Zhu 2000). For example, if there are six beam angles to be selected, NP_{size} can be set to 12 or a little more. Among these NP_{size} individuals, two strategies are used to implement the initialization: (1) some are initialized with equispaced angles with different rotations, and (2) the rest are randomly initialized. For example, if the beam number is 6 and the angle step is 10° for the discrete space of the whole 2π gantry angle, then the genes of the first individual are occupied by 0°, 60°, 120°, 180°, 240° and 300°, respectively, and 10°, 70°, 130°, 190°, 250° and 310°, respectively, for those of the second individual. Analogous operations are applied to the other four individuals, i.e. among the 12 individuals there are 6 individuals initialized with equispaced angles. Then the remaining six individuals are initialized randomly.

2.2.5. Definition of individual fitness. The quality of each individual is evaluated by a fitness value, and the purpose of optimization is to find the individual (i.e. a group of beam angles) with maximum fitness. The fitness value is calculated by

$$\text{Fitness}(\vec{s}) = F_{\max} - F_{\text{obj}}(\vec{s}) \qquad \vec{s} = \left(s_1, s_2, \ldots, s_{N_{\text{angle}}}\right). \tag{5}$$

Here $F_{\max}$ is a rough estimation of the maximum value of the objective function, $\vec{s}$ is a group of angles to be selected, and N_{angle} is the number of beam angles to be selected. Both $F_{\max}$ and $F_{\text{obj}}(\vec{s})$ are calculated using equations (1)–(4). Especially, $F_{\max}$ can be simply determined by setting it to be a little greater than the maximum objective function value of the individuals in the current generation, which ensures that all the fitness values are positive, a requirement of the selection operation to be mentioned below. It should be noted that the value

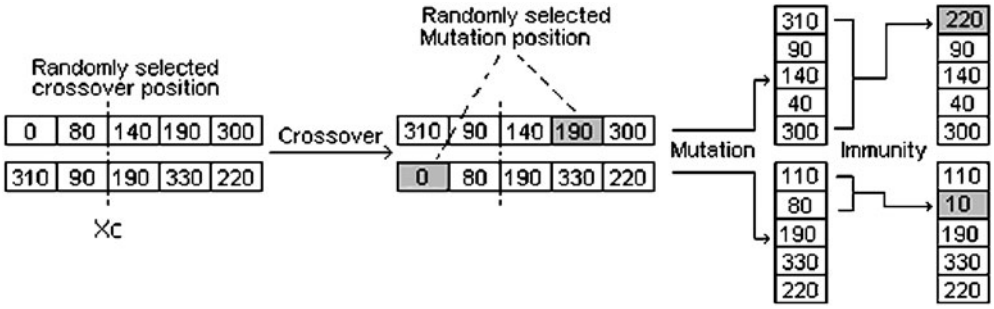

Figure 3. An illustration of genetic operations.

of $F_{\max}$ has no effect on the GA optimization, because there is a minus sign before $F_{\text{obj}}(\vec{s})$ in equation (5) and the minimum of $F_{\text{obj}}(\vec{s})$ always corresponds to the maximum of Fitness_i.

2.2.6. Fitness scaling. In order to enhance the performance of genetic progress, the following formulae are adopted to scale the fitness of each individual

$$\text{Fitness}_i = \exp(\text{Fitness}_i / T_k) \tag{6}$$

$$T_{k+1} = T_0 \cdot \lambda^k. \tag{7}$$

Here Fitness_i is the fitness of the ith individual in the kth generation, λ is a factor between (0, 1), normally 0.90 to 0.99, T_0 is a parameter called initial temperature. The idea of equation (7) is from the simulated annealing (SA) genetic algorithm, which aims to overcome premature convergence at the earlier stages of the evolution, or stalling at the later stages of the evolution.

Premature convergence is a problem often discovered in GA with small populations. At the start of a small population GA search it is common to have a few extraordinary individuals with a very high fitness in a population of mediocre individuals. These extraordinary individuals would take over a significant proportion of the population in a single generation. This would in turn lead to premature convergence and the optimal solution may not be found. The opposite phenomenon is apparent in the later stages of genetic progress. The average fitness of the population becomes very close to the maximum fitness of the population. This leads to the best members getting the same number of copies for reproduction as the mediocre members, and stalling the genetic evolution.

With equations (6) and (7), the few extraordinary chromosomes are scaled down while the lowly members of the population get scaled up. Also the difference of fitness values should be scaled up at the later stages because of the decreased temperature, which could make those best individuals more outstanding.

2.2.7. Genetic operations. There are four genetic operations adopted in this study, i.e. (1) selection, (2) crossover, (3) mutation and (4) immunity (figure 3). Parent individuals with higher fitness are selected into the next generation with a higher probability. To any two randomly selected parent individuals (angle sets), a crossover operation will be applied according to a specified crossover probability, normally 0.5–0.95. Then a mutation operation to the two children angle sets will be done according to a mutation probability, normally 0.001–0.02. Finally, an immunity operation is applied to the two children angle sets in order to enhance the genetic progress.

The selection probability of the ith individual, P_i, is determined according to a simple strategy of proportional fitness assignment expressed as (Goldberg 1989)

$$P_i = \frac{\text{Fitness}_i}{\sum_{j=1}^{NP_{\text{size}}} \text{Fitness}_j}. \tag{8}$$

After all the fitness values are calculated, a scheme called Roulette Wheel selection is used to determine which parent individual will be selected.

A crossover operation is illustrated in figure 3. The crossover positions X_c are randomly selected, and the two parts of the chromosome are exchanged with each other. After crossover two new chromosomes are generated: a chromosome with 310°, 90°, 140°, 190° and 300°, and another with 0°, 80°, 190°, 330° and 220°. The two new children will be selected as members of the new generation if their fitness values are greater than that of their parents, else their parents will be reserved.

If mutation can be done according to the mutation probability, this operation will be applied to a randomly selected gene of the two children individuals. The gene with 190° of the first new individual and the gene with 0° of the second new individual are randomly selected in figure 3. Then a choice is randomly made to determine which new angle will replace this selected gene. It should be noted that the new angle is required to be different from any of the existing angles in the chromosome. For example, the existing angles in the first chromosome are 310°, 90°, 140°, 190° and 300°, then the new angle used for mutation operation can be any one except these six angles. Here 40° is used to replace 190° for the first chromosome, and 110° to replace 0° for the second chromosome.

After mutation operation two new chromosomes are generated: a chromosome with 310°, 90°, 140°, 40° and 300°, and another with 110°, 80°, 190°, 330° and 220°. Then an operation called immunity will be applied to the two genes with 310° and 300° of the first chromosome and to the two genes with 110° and 80° of the second chromosome (figure 3), because we think that angles with 310° and 300° and angles with 110° and 80° are too close for a five-beam plan. Then one of the two angles of the first chromosome (randomly determined, here 310°) is randomly replaced with 220°, and one of the two angles of the second chromosome (80°) is randomly replaced with 10°.

The genetic operation will be terminated if there is no better individual found in a specified number of successive generations, and the individual with the highest fitness in the last generation will be regarded as the optimal set of beam angles.

2.3. Optimization of beam intensity maps using the conjugate gradient method

To each new individual an intensity map optimization is applied using the beam angles contained in the chromosome. The optimization is implemented fast using a CG method with the help of some special steps adopted to speed up the calculation. The final objective function value is saved to calculate the individual fitness.

The optimization of beam intensity maps has been studied by many researchers and a variety of algorithms have been published. These algorithms can be basically divided into two classes: (1) deterministic algorithm, such as gradient-based algorithm (including steepest descent, conjugate gradient and so on), maximum likelihood method and linear programming, and (2) stochastic algorithm, such as simulated annealing (SA) and GA. The stochastic algorithms have the powerful global searching ability, but the drawback of excessive computation time limits their clinical application. Gradient-based algorithms are fast, but have the potential to get trapped in local minima (Deasy 1997, Borgers and Quinto 1999,

Wu and Mohan 2002, Llacer *et al* 2003). Here a gradient-based algorithm is adopted considering the computation time.

The gradient-based algorithm used here is a conjugate gradient (CG) method similar to that adopted by Spirou and Chui (1998), which can be written as

$$\vec{x}^{(k+1)}(\lambda) = \vec{x}^{(k)} + \lambda \cdot \vec{h}^{(k+1)} \tag{9}$$

$$\vec{h}^{(k+1)} = -\nabla F_{\text{obj}}(\vec{x}^{(k+1)}) + \frac{[\nabla F_{\text{obj}}(\vec{x}^{(k+1)}) - \nabla F_{\text{obj}}(\vec{x}^{(k)})] \cdot \nabla F_{\text{obj}}(\vec{x}^{(k+1)})}{\nabla F_{\text{obj}}(\vec{x}^{(k)}) \cdot \nabla F_{\text{obj}}(\vec{x}^{(k)})} \cdot \vec{h}_k. \tag{10}$$

Here k means the kth iteration, $\vec{x}^{(k)}$ is the beam profile vector of the kth iteration, $\nabla F_{\text{obj}}(\vec{x}^{(k)})$ is the gradient of the objective function at the point $\vec{x}^{(k)}$, λ is the step size of the kth iteration, which can be easily calculated using a one-dimensional linear optimization, such as the golden section method. Equation (10) is initialized by setting $\vec{h}^{(1)} = -\nabla F_{\text{obj}}(\vec{x}^{(1)})$.

Mathematically, rays (i.e. beamlets) with negative weights will appear during the optimization of the intensity maps, which is not physically realizable. One common approach is to simply set the negative ray weights to zero at the end of each iteration. The problem with this approach is that the conjugate gradients of successive directions are no longer valid and there is no guarantee that an optimal solution will be found. To avoid this shortcoming, a method similar to Spirou and Chui (1998) is adopted in this paper. The non-negativity of ray weights is treated as a hard constraint that may not be violated under any circumstances. When the constraint prohibits the algorithm from taking the step λ that will make the objective function the minimum along the direction $\vec{h}$, the solution is to restart the recurrence relation of equations (9) and (10) from the current point.

The optimization of intensity maps is terminated when $(F_{\text{obj}}(\vec{x}^{(k)}) - F_{\text{obj}}(\vec{x}^{(k-1)}))/F_{\text{obj}}(\vec{x}^{(k)})$ is less than a sufficiently small value (0.001 is used in this study) after the kth iteration.

2.4. Dose calculation

In our study, the dose calculation is based on a pencil-beam-based three-dimensional full scatter convolution (FSC) algorithm, in which both the scatter effects and tissue heterogeneity correction are involved. For all the discrete angle candidates, the doses at each point contributed by each pencil beam, called dose deposition matrices, are previously calculated for all volumes before the optimization. The corresponding matrices are used if some beam angles are selected by GA during the optimization. To speed up the calculation, two main measures are adopted: (1) only the doses of those pencil beams in the BEV of the target are calculated, we called them effective rays, and (2) the deposition matrices are indexed so that only a very small number of point doses that exceed a specified threshold value will participate in the dose calculation because these matrices are very sparse. With the optimal beam angles, a refined intensity map optimization is applied and a final dose calculation is done using the non-indexed deposition matrices.

3. Results and discussion

In order to verify the presented ABAS technique, first two simulated phantom cases (test cases A and B) with obvious optimal beam angles are carefully selected to see if ABAS can find the optimal beam angles. Then a more complicated phantom case (test case C) simulating a prostate tumour is used to test the efficiency of ABAS. Finally, two clinical tumour cases

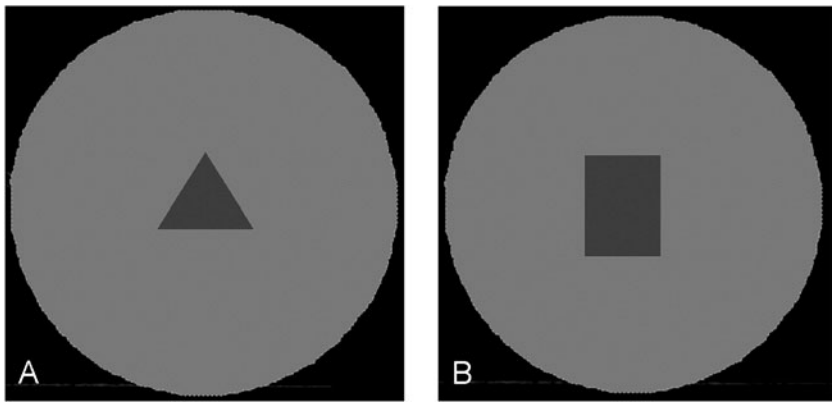

Figure 4. Two simulated cases with known optimal beam angles. For case A, two groups of angles, 30°, 150° and 270°, or 90°, 210° and 330°, are the known optimal angles if three beams are used, and 0°, 90°, 180° and 270° for case B if four beams are selected.

are used to demonstrate the advantage of ABAS again. All the tests are done on a personal computer (AMD athlon(tm) MP 1800+, 1.53 GHz, 512 MB RAM).

3.1. Test cases A and B

The two simulated cases shown in figure 4 are used to test the validity of ABAS. For case A two groups of angles, 30°, 150° and 270° or 90°, 210° and 330°, are the known optimal angles if three beams are used, and 0°, 90°, 180° and 270° for case B if four beams are selected. It should be noted that, because these known optimal angles are equispaced, here we only randomly initialize those individuals in the first generation and do not initialize them with equispaced angles, in order to fully test the validity of ABAS. The whole 2π gantry angle is sampled with a discrete angle step of 5°, and no beam angle constraint is added. Thus there are 72 discrete angles in the candidate pool.

As expected, the optimal angles for these two cases are found after a time of less than 5 min. The optimized beam angles and the dose distributions are shown in figure 5. The optimized beam angles are 30°, 150° and 270° for case A, and 0°, 90°, 180° and 270° for case B, the same as the known ones. It should be noted that the transverse dose distributions of both cases are not symmetrical because the isocentres of the two cases are not the exact centres of the two phantoms.

3.2. Test case C

A more complicated case simulating a prostate tumour is used to test the efficiency of ABAS. The simulated case includes a prostate (PTV) with a concave outline with adjoining organs at risk (OARs), bladder and rectum (figure 6). In this phantom case, volumes occupy 10 CT slices and the contours of volumes are the same on different slices. The dose prescription to the PTV is set to 73 Gy, which is normalized to 100%. The CT slice intervals are 0.5 cm, and the size of the voxel volume is set to 0.5 cm $\times$ 0.5 cm $\times$ 0.5 cm for all of the volumes. The pencil beam size is 0.5 cm $\times$ 0.5 cm at the isocentre plane. Five coplanar 6 MV photon beams are used to irradiate the PTV. The case is optimized using both pre-defined equispaced beams and auto-selected beams using ABAS.

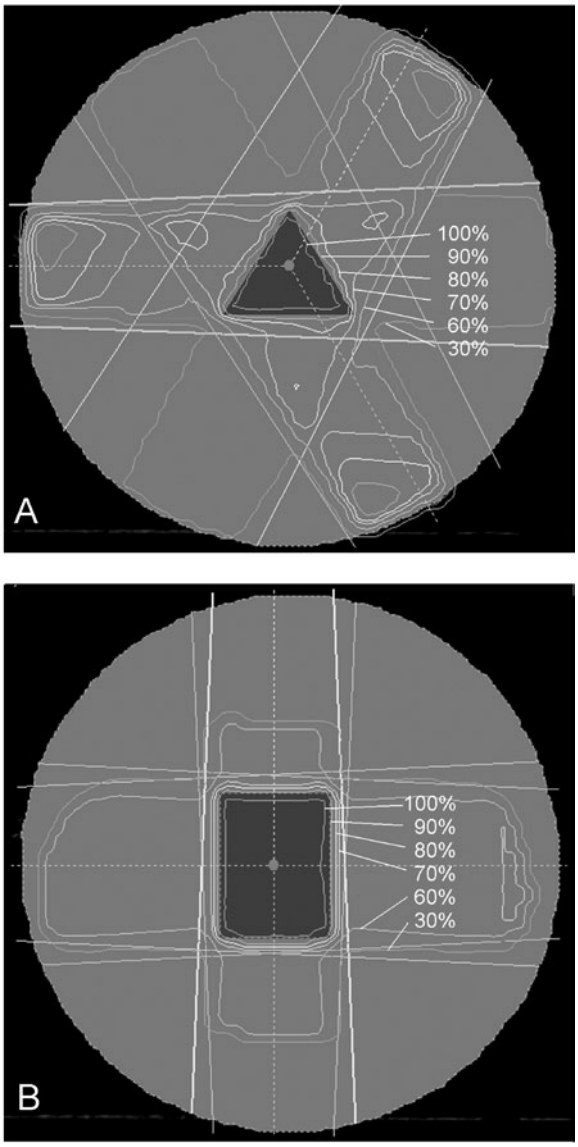

Figure 5. The optimized beam angles and dose distributions using ABAS. The optimized beam angles are 30°, 150° and 270° for case A, and 0°, 90°, 180° and 270° for case B.

The angles of those five pre-defined equispaced beams are 0°, 72°, 144°, 216° and 288°. The beam set-up and the dose distribution are shown in figure 6(A). As for the optimization using ABAS, an angle step of 5° is used and no beam orientation constraint is applied. After a 13 min optimization, the final optimized angles are found: 0°, 70°, 130°, 240° and 295°. The beam set-up and dose distribution are shown in figure 6(B). The comparison of dose–volume histograms (DVHs) is shown in figure 7. Both of the dose distributions and DVHs show the improvements given by ABAS: a more uniform dose for PTV and lower doses for bladder and rectum. There are two main reasons to explain why the optimized beam set-up is not

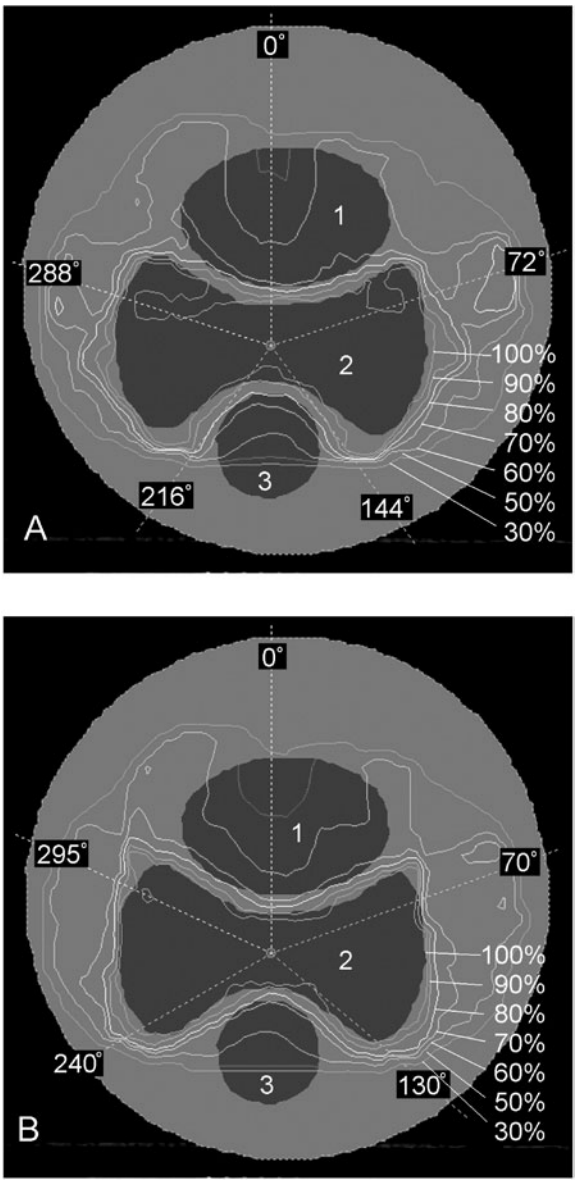

Figure 6. A more complicated case simulating the prostate tumour, including a prostate (PTV) with a concave outline with adjoining organs at risk (OARs), bladder and rectum. Cases A and B are the beam angles and dose distributions using five equispaced beams and optimized angles with ABAS, respectively.

symmetrical: one is that not all of the three volumes are symmetrically located in the phantom, and another is that the PTV is not itself symmetrical.

3.3. Spine case

Figure 8 shows a clinical case with a spine tumour with adjoining OAR (spinal cord). The dose constraint added to PTV is a minimum dose of 75 Gy. The constraints applied to the OAR are

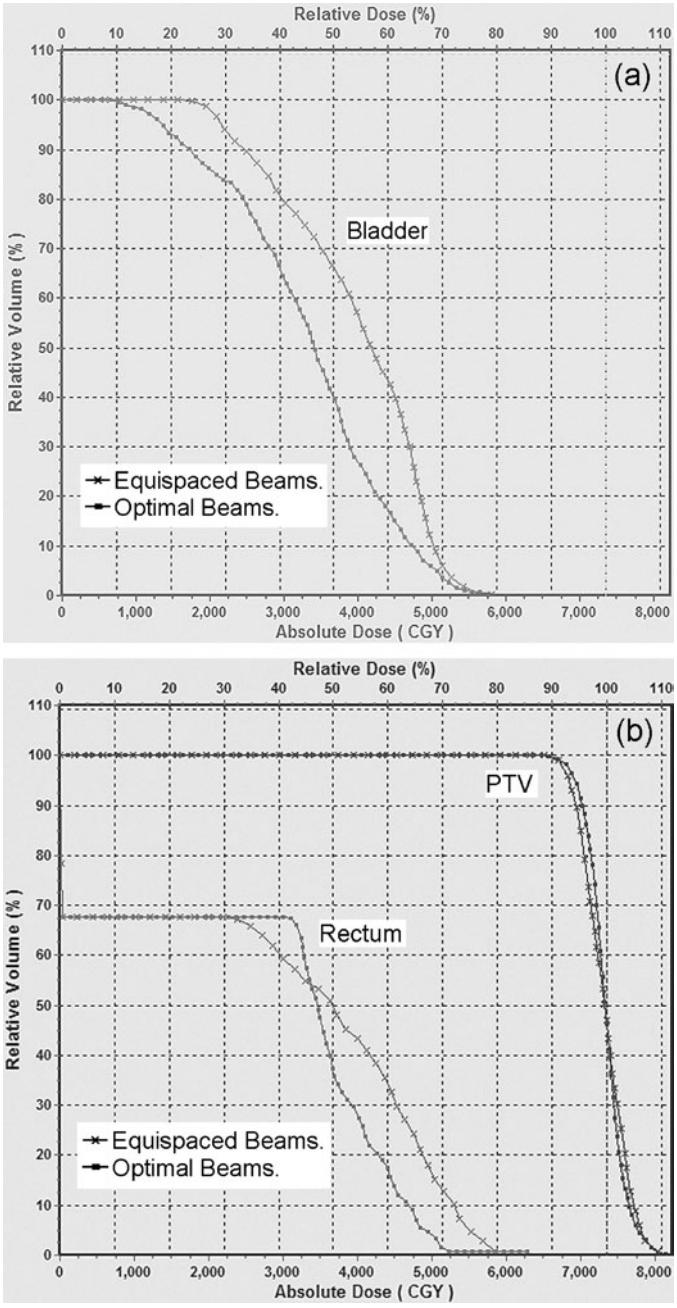

Figure 7. DVH comparison of test case C shown in figure 6.

a maximum dose of 50 Gy, with no more than 50% of the OAR volume receiving more than 20 Gy. The dose prescription to the PTV is set to 75 Gy, which is normalized to 100%. The CT slice intervals are 0.5 cm, and the size of the voxel volume is set to 0.3 cm $\times$ 0.3 cm $\times$ 0.5 cm for both the PTV and OAR because of the small volumes. The pencil beam size is 0.5 cm $\times$ 0.5 cm at the isocentre plane. Five coplanar 6 MV photon beams are used to irradiate

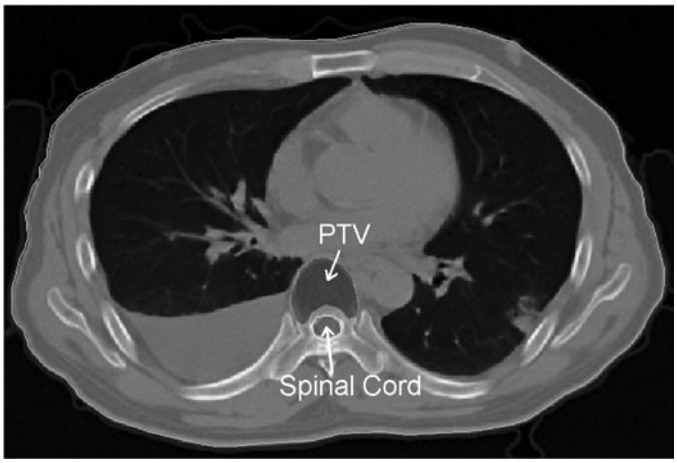

Figure 8. A clinical case with spine tumour with adjoining OAR (spinal cord).

the PTV. Similar to test case C, this case is optimized using both pre-defined equispaced beams and auto-selected beams using ABAS.

The angles of the five pre-defined equispaced beams are 0°, 72°, 144°, 216° and 288°. The corresponding beam set-up and the final dose distribution are shown in figure 9(A). As for the optimization using ABAS, an angle step of 10° is used and no beam orientation constraint is applied. After a 19 min optimization, the final optimized angles are found: 20°, 100°, 170°, 240° and 310°. The optimal beam set-up and the corresponding dose distribution are shown in figure 9(B). The comparison of dose–volume histograms (DVHs) is shown in figure 10. From the DVHs we can see that the OAR receives a lower dose for the plan using optimal beam angles, compared with that using equispaced beams, under the condition of a slightly more uniform dose in PTV. This is also demonstrated in dose distributions: most of the OAR is outside the 50% iso-dose line for the plan with optimal beams (figure 9(B)).

3.4. Prostate case

A more complicated clinical case is shown in figure 11, in which a prostate (PTV) is surrounded by four OARs: bladder, rectum, left femur head and right femur head. The sizes and relative positions of the volumes change substantially from slice to slice, and on most of the slices the contours of the rectum and bladder overlap with the PTV. Figures 11(a) and (c) show the volume structures on two different slices: slice position with 0.0 cm and 2.5 cm. The CT slice intervals are 0.5 cm, the size of the voxel volume is set to 0.5 cm × 0.5 cm × 0.5 cm for PTV, bladder, left and right femur heads, and 0.3 cm × 0.3 cm × 0.5 cm for the rectum, because of the relatively small volume size. The dose prescription to the PTV is set to 76 Gy, which is normalized to 100%.

Optimization with seven beams is studied, and the results of ABAS are compared with those of a manual plan with a set of seven coplanar beams with angles of 0°, 50°, 100°, 150°, 210°, 260° and 310° (figures 11(a) and (c)), which has become an informal standard for beam set-up for prostate cases. With the same optimization parameters, the case is also optimized using the ABAS method. For ABAS, a small angle step of 5° is used and no beam orientation constraint is applied. After a relatively long 36 min optimization, the final optimized angles are found: 10°, 60°, 110°, 155°, 200°, 250° and 300° (figures 11(b) and (d)).

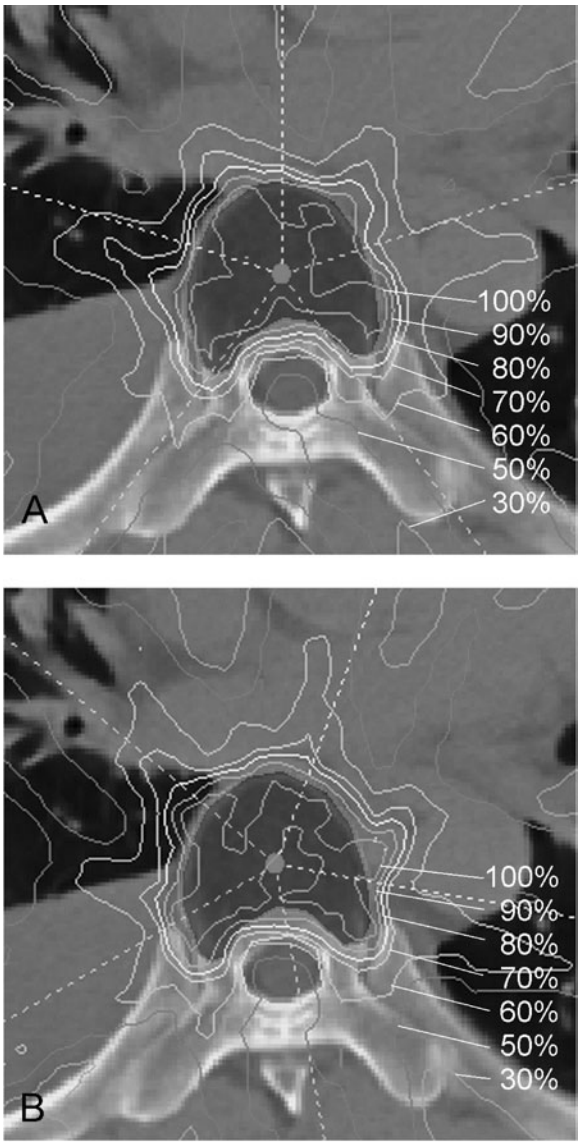

Figure 9. The dose distributions of the spine case shown in figure 8. In case A five pre-defined equispaced beams with 0°, 72°, 144°, 216° and 288° are used. In case B five angles with 20°, 100°, 170°, 240° and 310° are derived from ABAS.

The dose distributions of the manual plan on two different slices are displayed in figures 11(a) and (c), and the corresponding dose distributions of ABAS are shown in figures 11(b) and (d). From these dose distributions we can see that, with a higher conformality, the PTV in ABAS is more tightly surrounded by high doses, and the OARs are spared high doses for larger volumes, especially for the rectum, compared to the dose distributions of the manual plan. The DVH comparisons in figure 12 also demonstrate the better results of ABAS. Even the DVH of PTV of the manual plan is a little better than that of the ABAS plan, but there is no obvious difference between them. As for the four OARs, the DVHs of ABAS are much

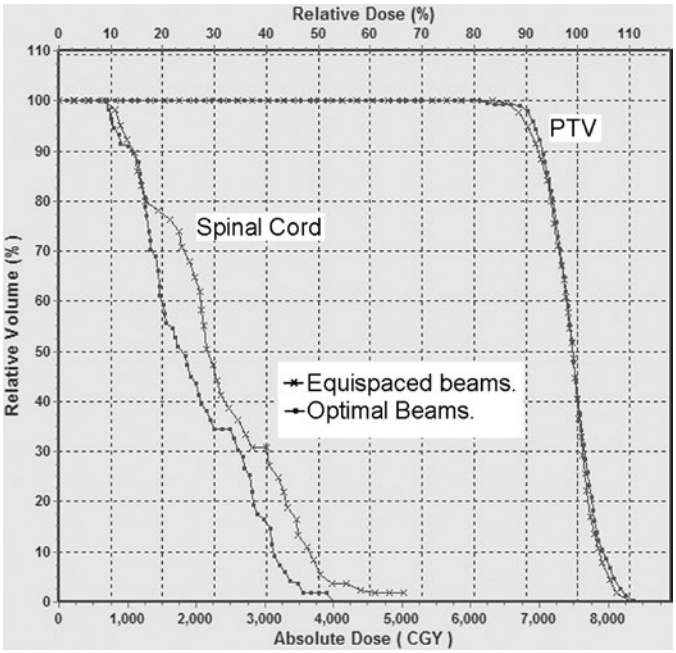

Figure 10. DVH comparison of the clinical case shown in figures 8 and 9.

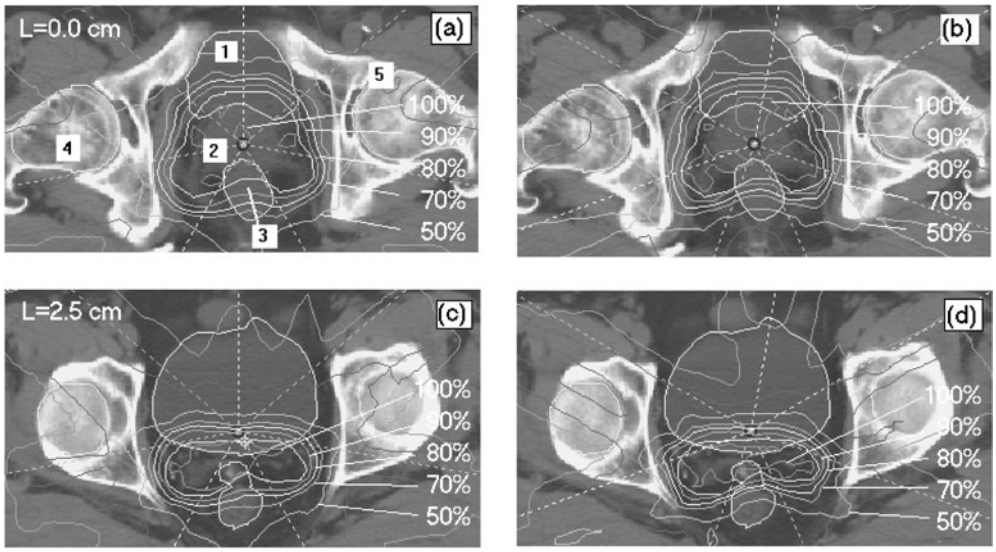

Figure 11. The volume structures and dose distributions of the prostate case. There are a total of five volumes involved: 1—bladder, 2—PTV (prostate), 3—rectum, 4—right femur head, 5—left femur head. The straight dotted lines and solid dose lines on (a) and (c) represent the beam directions (0°, 50°, 100°, 150°, 210°, 260° and 310°) and dose distributions of the manual plan, the straight dotted lines and solid dose lines on (b) and (d) represent the beam directions (10°, 60°, 110°, 155°, 200°, 250° and 300°) and dose distributions of the ABAS plan. (a) and (b) show the slice with position 0.0 cm, and (c) and (d) show the slice with position 2.5 cm.

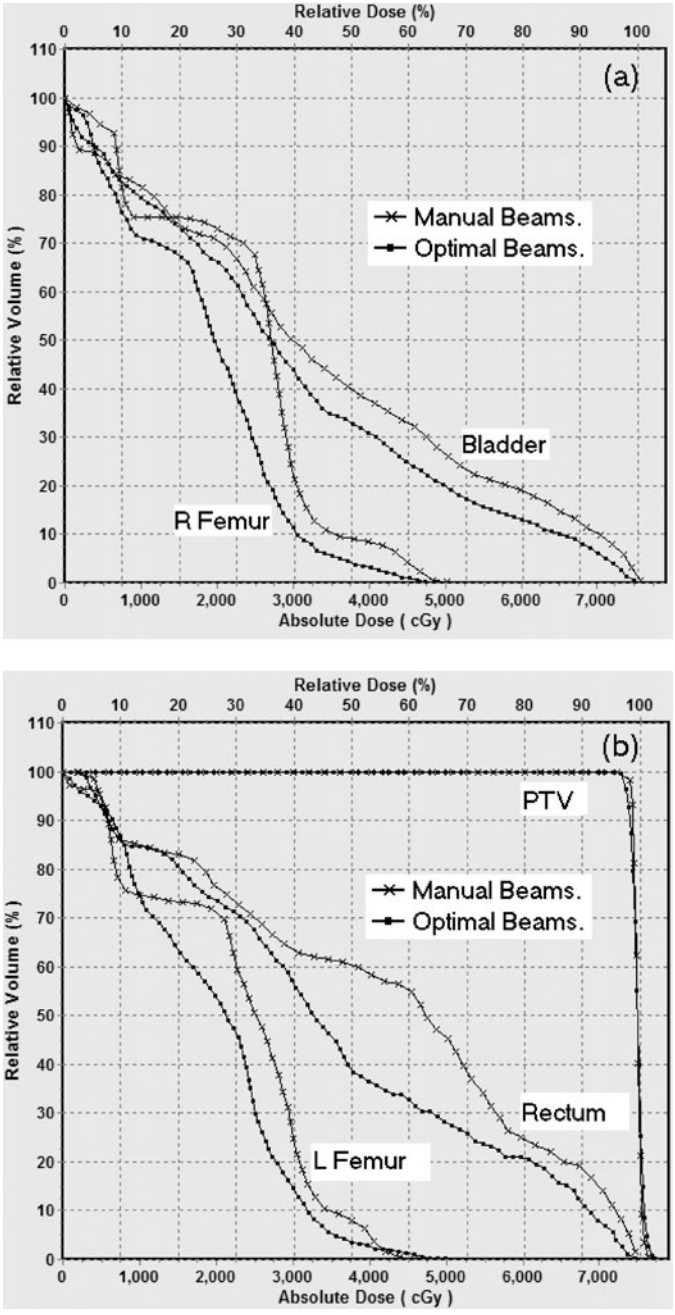

Figure 12. DVH comparison of the manual plan and the optimized plan for the prostate shown in figure 11, (a) for right femur and bladder, and (b) for PTV, rectum and left femur.

better than that of the manual plan. There is no big difference in beam directions between the manual plan and the ABAS plan, whereas ABAS gives much better dose distributions, one of the main reasons may be the complicated anatomy structures: PTV with a concave outline with adjoining OARs (rectum and bladder), even overlapping with each other.

4. Conclusions

In this paper, an efficient IMRT tool is developed to automatically select beam angles for inverse planning. In our automatic beam angle selection (ABAS) algorithm, the selection of beam angles and the optimization of intensity maps are treated as two separate processes and implemented iteratively. A genetic algorithm (GA) is used to select suitable beam angles, and a conjugate gradient (CG) method is used to fast optimize intensity maps for each selected beam combination based on a dose-based objective function. A pencil-beam-based three-dimensional (3D) full scatter convolution (FSC) algorithm is employed for the dose calculation. In section 3, two simulated cases with obvious optimal beam angles are used to verify the validity of the presented technique, and a more complex case simulating a prostate tumour and two clinical cases are employed to test the efficiency of ABAS. Both of the DVHs and dose distributions show that ABAS is valid and efficient and can improve the dose distributions.

In order to implement the beam angle optimization within a clinically acceptable computation time, some special tricks are adopted to enhance the optimization efficiency: (1) the objective function is simplified during beam angle selection, and the whole complicated function is only used for the optimization of final intensity maps, (2) an immunity operation is incorporated in GA, and (3) a useful fitness-scaling process is done in order to improve the genetic progress. We think that GA is very suitable for the optimization of beam angles, for it can provide an effective crossover and mutation operation and no decoding operation is needed for the calculation of individual fitness.

In this paper, we have assumed that the number of beams was previously defined by a planner before beam angle optimization. A disadvantage is that several trial-and-error tests may be needed to specify a suitable beam number if a complicated case is hoped to be treated using a very small number of beams. The choice of the optimal number of beams represents another important issue in IMRT planning (Pugachev and Xing 2002), which is a work that should be addressed in further research with much effort, even though it has been studied by many researchers (Soderstrom and Brahme 1995, Stein *et al* 1997).

The beams in this study are restricted to coplanar ones. It should be noted that the algorithm could be easily extended to non-coplanar beam angle selection by just adding a couch angle variable in the optimization scheme, with the sacrifice of a longer computation time. Of course, a better dose distribution may be potentially acquired by using a smaller number of beams with non-coplanar angles.

The main limitation of the automatic beam angle selection algorithm is the long computation time in order to find the optimal results. At the same time, the plentiful experience in selecting beam angles that physicists and oncologists have accumulated cannot be utilized during the beam angle optimization. In section 2.2.3 a useful tool is provided which can be utilized by those experienced planners. By defining enough beam angle constraints, planners can reserve the orientations that beams may pass through with highest probability, according to their experience. With this tool, not only the optimization time will be saved because of the reduction of the search space, but also the accumulated experience of the physicists and oncologists can be incorporated into the optimization.

As a powerful IMRT tool, ABAS has been embedded in the anti-tumour radiation treatment planning (ARTP) system (Topslane Inc., Pleasant Hill, CA, USA) for routine use. We are currently working on: (1) building a knowledge database to guide the beam angle selection in order to fully utilize the accumulated experience in manual selection of beam angles (Xing *et al* 1999, Pugachev and Xing 2002), and (2) implementing GA through parallel computation on a PC with dual or more CPUs.

Acknowledgments

This work is supported by a grant from NSFC of China, grant no 90208003, a grant from the Doctor Training Fund of the Ministry of Education (MOE), China, and a grant from TRAPOYT of China, and also partially supported by Topslane Inc. The authors would like to thank Wenyan Chen, Lin Feng, Jiancheng Zheng and Dongmei Lu of Topslane for their helpful discussions and assistance.

References

Borgers C and Quinto E T 1999 On the non-uniqueness of optimal radiation treatment plans *Inverse Problems* **15** 1115–38

Bortfeld T and Schlegel W 1993 Optimization of beam orientation in radiation therapy: some theroretical considerations *Phys. Med. Biol.* **38** 291–304

Deasy J O 1997 Multiple local minima in radiotherapy optimization problems with dose–volume constraints *Med. Phys.* **24** 1157–61

Goldberg D E 1989 *Genetic Algorithms in Search, Optimization, and Machine Learning* (Reading, MA: Addison-Wesley)

Ezzell G A 1996 Genetic and geometric optimization of three-dimensional radiation therapy treatment planning *Med. Phys.* **23** 293–305

Haas O C L, Burnham K J and Mills J A 1998 Optimization of beam orientation in radiotherapy using planar geometry *Phys. Med. Biol.* **43** 2179–93

Langer M *et al* 1996 A generic genetic algorithm for generating beam weights *Med. Phys.* **23** 965–71

Llacer J, Deasy J O, Bortfeld T R, Solberg T D and Promberger C 2003 Absence of multiple local minima effects in intensity modulated optimization with dose–volume constraints *Phys. Med. Biol.* **48** 183–210

Pugachev A B, Boyer A L and Xing L 2000 Beam orientation optimization in intensity-modulated radiation treatment planning *Med. Phys.* **27** 1238–45

Pugachev A B and Xing L 2002 Incorporating prior knowledge into beam orientation optimization in IMRT *Int. J. Radiat. Oncol. Boil. Phys.* **54** 1565–74

Rowbottom C G, Khoo V S and Webb S 2001 Simultaneous optimization of beam orientations and beam weights in conformal radiotherapy *Med. Phys.* **28** 1696–702

Rowbottom C G, Webb S and Oldham M 1998a Improvement in prostate radiotherapy from the customization of beam directions *Med. Phys.* **25** 1171–9

Rowbottom C G, Webb S and Oldham M 1998b Beam-orientation customization using an artificial neural network *Phys. Med. Biol.* **44** 2251–62

Spirou S V and Chui C S 1998 A gradient inverse planning algorithm with dose–volume constraints *Med. Phys.* **25** 321–33

Soderstrom S and Brahme A 1992 Selection of suitable beam orientation in radiation therapy using entropy and Fourier transform measures *Phys. Med. Biol.* **37** 911–24

Soderstrom S and Brahme A 1995 Which is the most suitable number of photon beam portals in coplanar radiation therapy? *Int. J. Radiat. Oncol. Boil. Phys.* **33** 151–9

Stein J, Mohan R, Wang X H, Bortfeld T, Wu Q W, Preiser K, Ling C C and Schlegel W 1997 Number and orientations of beams in intensity-modulated radiation treatments *Med. Phys.* **24** 149–60

Webb S 2000 *Intensity-Modulated Radiation Therapy* (Bristol: Institute of Physics Publishing)

Woudstra E and Storchi P R M 2000 Constrained treatment planning using sequential beam selection *Phys. Med. Biol.* **45** 2188–49

Wu Q and Mohan R 2002 Multiple local minima in IMRT optimization based on dose–volume criteria *Med. Phys.* **29** 1514–27

Wu X and Zhu Y 2000 A mixed-encoding genetic algorithm with beam constraint for conformal radiotherapy treatment planning *Med. Phys.* **27** 2508–16

Wu X and Zhu Y 2002 A maximum-entropy method for the planning of conformal radiotherapy *Med. Phys.* **29** 2241–6

Xing L *et al* 1999 A medical knowledge based system for the selection of beam orientations in intensity modulated radiation therapy (IMRT) *Int. J. Radiat. Oncol., Biol. Phys.* **45** (Suppl. 1) 246–7

Yu Y and Schell M C 1996 A genetic algorithm for the optimization prostate implants *Med. Phys.* **23** 2085–91

Zhang P *et al* 2001 Optimization of gamma knife treatment planning via guided evolutionary simulated annealing *Med. Phys.* **28** 1746–52